Experimental Hematology

Experimental Hematology 2019;73:50–63

REGULAR SUBMISSION

ETV6-RUNX1 interacts with a region in *SPIB* intron 1 to regulate gene expression in pre-B-cell acute lymphoblastic leukemia

Li S. Xu[a,b], Alyssa Francis[a], Shereen Turkistany[c], Devanshi Shukla[a], Alison Wong[a], Carolina R. Batista[a,b], and Rodney P. DeKoter[a,b]

[a]*Department of Microbiology & Immunology and the Centre for Human Immunology, Schulich School of Medicine & Dentistry, Western University, London, ON, Canada;* [b]*Division of Genetics and Development, Children's Health Research Institute, Lawson Research Institute, London, ON, Canada;* [c]*Center of Innovation in Personalized Medicine, Jeddah, Saudi Arabia*

(Received 19 July 2018; revised 28 March 2019; accepted 30 March 2019)

The most frequently occurring genetic abnormality in pediatric B-lymphocyte-lineage acute lymphoblastic leukemia is the t(12;21) chromosomal translocation that results in a *ETV6-RUNX1* (also known as *TEL-AML1*) fusion gene. Expression of ETV6-RUNX1 induces a preleukemic condition leading to acquisition of secondary driver mutations, but the mechanism is poorly understood. SPI-B (encoded by *SPIB*) is an important transcriptional activator of B-cell development and differentiation. We hypothesized that *SPIB* is directly transcriptionally repressed by ETV6-RUNX1. Using chromatin immunoprecipitation, we identified a regulatory region in the first intron of *SPIB* that interacts with ETV6-RUNX1. Mutation of the RUNX1 binding site in *SPIB* intron 1 prevented transcriptional repression in transient transfection assays. Next, we sought to determine to what extent gene expression in REH cells can be altered by ectopic SPI-B expression. SPI-B expression was forced using CRISPR-mediated gene activation and also using a retroviral vector. Forced expression of SPI-B resulted in altered gene expression and, at high levels, impaired cell proliferation and induced apoptosis. Finally, we identified *CARD11* and *CDKN1A* (encoding p21) as transcriptional targets of SPI-B involved in regulation of proliferation and apoptosis. Taken together, this study identifies *SPIB* as an important target of ETV6-RUNX1 in regulation of B-cell gene expression in t(12;21) leukemia.

Acute lymphoblastic leukemia (ALL) is the most frequently occurring type of cancer in young children. Despite a better than 90% cure rate, ALL is still the leading cause of leukemia-related deaths in children [1]. Eighty percent of pediatric ALLs are cancers of the B-lymphocyte lineage (B-ALL), and two-thirds of these involve mutation or chromosomal translocation of genes encoding transcription factors [2]. The most frequently occurring genetic abnormality in pediatric B-ALL is the t(12;21) chromosomal translocation that results in an *ETV6-RUNX1* (also known as *TEL-AML1*) fusion gene [3]. This occurs in 22% of patients [1]. ETV6 and RUNX1 are transcription factors that normally function as transcriptional activators during B-cell development. Fusion of a portion of ETV6 to the DNA binding domain of RUNX1 results in altered activity and transcriptional reprogramming of affected cells [4]. Ectopic expression of ETV6-RUNX1 in mice is not sufficient to drive leukemogenesis by itself, but strongly cooperates with various mutations to induce leukemia [5,6]. For example, an insertional mutagenesis screen demonstrated that mutation of genes important for transition through pro-B− and pre-B−cell stages of development, including

Offprint requests to: Rodney P. DeKoter, Department of Microbiology & Immunology, Schulich School of Medicine & Dentistry, Western University, London, ON, Canada N6A 5C1; E-mail: rdekoter@uwo.ca

Supplementary material associated with this article can be found in the online version at https://doi.org/10.1016/j.exphem.2019.03.004.

0301-472X/
https://doi.org/10.1016/j.exphem.2019.03.004

SPIB, cooperated with ETV6-RUNX1 to induce B-ALL [6].

SPI-B (encoded by *SPIB*) is a transcription factor of the ETS family that is highly related to the myeloid and B-cell transcriptional regulator protein PU.1 (encoded by *SPI1*). SPI-B is an important transcriptional activator of genes encoding proteins functioning in the B-cell receptor (BCR) signaling pathway [7–10]. Deletion of *Spib* cooperates with deletion of *Spi1* to induce B-ALL at 100% incidence in mice [11,12]. Disruption of *Spib,* using a *Sleeping Beauty* transposase screen, shows that mutagenesis of *Spib* strongly cooperates with ETV6-RUNX1 in mice to induce B-ALL [6]. Therefore several lines of evidence suggest that SPI-B is a tumor suppressor for B-ALL.

SPIB is directly activated by RUNX1 during B-cell development [13]. *SPIB* mRNA transcript levels are expressed at low levels in 12;21 (ETV6-RUNX1) leukemia relative to other leukemia subtypes, and at low levels compared with normal human pre-B cells [14]. When RNA interference was used to knock down ETV6-RUNX1 in REH and AT-2 cell lines carrying the 12;21 translocation, *SPIB* was the top upregulated gene [15]. These results suggest that *SPIB* is an important target gene that is transcriptionally repressed by ETV6-RUNX1 in developing B cells carrying the 12;21 translocation.

We hypothesized that *SPIB* is directly transcriptionally repressed by ETV6-RUNX1. To test this hypothesis, we investigated transcriptional regulation of *SPIB* in a human ETV6-RUNX1 cell line, REH. We identified a regulatory region in the first intron of *SPIB* that interacts with ETV6-RUNX1. Mutagenesis of the RUNX1 binding site in *SPIB* intron 1 prevented transcriptional repression in transient transfection assays. Next, we sought to determine to what extent gene expression in REH cells could be altered by ectopic SPI-B expression. SPI-B expression was forced using a retroviral vector and also from the endogenous locus using CRISPR-mediated gene activation. Depending on the level of expression, forced expression of SPI-B resulted in altered gene expression, impaired cell proliferation, and apoptosis. Finally, we identified *CARD11* and *CDKN1A* (encoding p21) as transcriptional targets of SPI-B involved in regulation of proliferation and apoptosis. Taken together, this study identifies *SPIB* as an important target of ETV6-RUNX1 in programming of B-cell gene expression in t (21;21) leukemia.

Methods

Cell culture and flow cytometry

REH cells [16] were obtained from the American Type Culture Collection (ATCC, Manassas, VA) and were maintained in complete ATCC-formulated RPMI-1640 medium (Wisent, St. Bruno, QC, Canada). OCI-LY3 cells [17] were maintained in Iscove's modified Dulbecco's medium (IMDM, Wisent). Complete medium was supplemented with 10% bovine serum (Wisent), $1\times$ penicillin/streptomycin/L-glutamine (Wisent), and 5×10^{-5} mol/L β-mercaptoethanol (βME) (Sigma-Aldrich, St. Louis, MO). Flow cytometry analysis was performed using an FACSCanto (BD Biosciences, Franklin Lakes, NJ), and cell sorting was performed using a FACSAria III (BD Biosciences). Proliferation assays were performed using CellTrace Violet (Thermo-Fisher) according to the manufacturer's instructions. Flow cytometry analysis was performed using FlowJo 10 (TreeStar, Ashland, OR).

Luciferase assays

REH cells were electroporated using the Bio-Rad Gene Pulser II with capacitance extender (Bio-Rad, Mississauga, ON, Canada) at settings of 220 V and 950˚F. LY3 cells were electroporated at settings of 170 V and 950˚F. Five million cells were electroporated with 10 μg pGL3-based reporter plasmid DNA and 0.5 μg pRL-TK control plasmid (Promega, Madison, WI). Twenty-four hours after electroporation, cells were lysed with passive lysis buffer, and firefly and renilla luciferase activity was measured using a Dual Luciferase Assay reagent kit (Promega) and a Biotek Cytation 5 imaging reader (BioTek, Winooski, VT).

Chromatin immunoprecipitation analysis

REH cells were cross-linked with formaldehyde for 10 min at room temperature. Crosslinked cells were neutralized with 125 mmol/L glycine, then washed with cold phosphate-buffered saline. Fixed cells were lysed with buffer (50 mmol/L Tris-HCl [pH 8.1], 10 mmol/L EDTA, 1% sodium dodecyl sulfate [SDS]) containing HALT protease inhibitors (Thermo-Fisher). Samples were sonicated using a Bioruptor instrument (Diagenode, Denville, NJ) to an average DNA size of 200–1,000 bp. Sonicated chromatin was incubated with rabbit anti-RUNX1, or control rabbit anti-IgG (ChIP grade, ABCAM), which were coupled to protein G Dyna-Beads overnight at 4˚C. Beads were washed once with low-salt wash buffer (0.1% SDS, 1% Triton X-100, 2 mmol/L EDTA, 20 mmol/L Tris-Cl, 150 mmol/L NaCl). Then, beads were washed once with high-salt buffer (0.1% SDS, 1% Triton X-100, 2 mmol/L EDTA, 20 mmol/L Tris–HCl, 500 mmol/L NaCl). Next, beads were washed with LiCl buffer (0.25 mol/L LiCl, 1% Nonidet P-40, 1% Na deoxycholate, 1 mmol/L EDTA, 10 mmol/L Tris-Cl). Finally, beads were washed twice with Tris-EDTA buffer at pH 8. After washing, antibody, beads, and chromatin complex were eluted with elution buffer (1% SDS, 0.1 mol/L $NaHCO_3$). Eluted solution was incubated at 65˚C overnight to reverse cross-linking. DNA was purified using the Qia-Quick PCR purification kit (Qiagen, Toronto, ON, Canada). Quantitative polymerase chain reaction (PCR) was used to measure the fold enrichment and percentage input enrichment of the immunoprecipitated DNA using specific primers designed to amplify the predicted RUNX1 binding sites (Supplementary Table E1, online only, available at www.exphem.org).

Immunoblot analysis

Whole-cell lysates were prepared using Laemmli buffer, resolved by sodium dodecyl sulfate–polyacrylamide gel electrophoresis (SDS-PAGE), and transferred to nitrocellulose (Thermo-Fisher). Immunoblotting was performed using rabbit anti-SPI-B (a kind gift from Dr. Reuben Tooze), horseradish peroxidase (HRP)-conjugated mouse monoclonal anti-FLAG (M2, Sigma-Aldrich), rabbit polyclonal anti-CAS9 (Santa Cruz SC-392737, Santa Cruz, CA), or HRP-conjugated rabbit polyclonal anti-actin (Santa Cruz SC-47778). Secondary antibodies included HRP-conjugated anti-rabbit or HRP-conjugated goat anti-rabbit IgG (Santa Cruz SC-2004). Immunoblots were visualized with Supersignal West Pico reagent (Thermo-Fisher) and Amersham HyperFilm ECL (GE Healthcare Inc., Mississauga, ON, Canada).

Quantitative polymerase chain reaction

RNA was prepared using an RNEasy kit (Qiagen) and employed to synthesize cDNA using an iSCRIPT kit and random priming (Bio-Rad). Quantitative real-time reverse transcription PCR (RT-qPCR) was performed using SensiFAST SYBRGreen Supermix (Bioline, Taunton, MA) and an Applied Biosystems QuantStudio 5 thermal cycler (Thermo-Fisher). Absolute quantitation of PCR for *SPIB* and *GAPDH* was determined by interpolation based on a standard curve generated from a dilution series of plasmid of known concentration. Primers used to amplify segments of the *SPIB* and *GAPDH* cDNA, as well as all primers used for RT-qPCR or qPCR analysis, are described in Supplementary Table E1.

Plasmid construction

A 469-bp fragment of *SPIB* intron 1 and a 921-bp fragment of the *SPIB* promoter were amplified by PCR from REH cell genomic DNA and cloned using a PCR cloning kit (Agilent, Santa Clara, CA) before ligation into pGL3-basic or pGL3-promoter vectors (Promega, Madison, WI) using standard cloning techniques. pU6-sgRNA-CXCR4 and lenti-dCAS9-VP64 lentiviral vectors [18] were obtained from AddGene. Single guide RNA sequences were designed using the Zhang lab CRISPR design tool [19]. The Q5 site-directed mutagenesis kit (New England Biolabs, Ipswich, MA) was used to delete CXCR4 synthetic guide RNA (sgRNA) sequence to generate pU6-sgRNA and to insert sgRNA sequences directed to the *SPIB* promoter into pU6-sgRNA, as well as to perform site-directed mutagenesis. pLVX-EF1α-ZsGreen lentiviral vector was obtained from TaKaRa Bio (Mountain View, CA). Lentiviral vectors encoding 3XFLAG-tagged human SPI-B (pLVX-hSPIB) and PU.1 (pLVX-hPU.1), as well as mutants that are unable to bind DNA (pLVX-hSPIB R229,232A or pLVX-hPU.1 R230,233A), were constructed using standard cloning techniques. All primers used for PCR are described in Supplementary Table E1.

Lentiviral production

Lentiviral packaging was performed with HEK-293T packaging cells transfected using PEIPro reagent (PolyPlus, New York, NY). Cells at 80% confluence in 10-cm tissue culture dishes were transfected with 24 μg total plasmid DNA including lentiviral vector, pDR8.2, and pMD2 vectors encoding gag, pol, and VSVg env. Virus-containing supernatants were collected 48 hours after transfection. Infections were performed using spinoculation of 10^6 cells with 1 mL virus-containing supernatant in the presence of 4 μg/ml polybrene for 2 hours at 3,000*g*. Infection frequencies were determined by flow cytometry at 48 hours.

Bioinformatic analyses

Previously published Affymetrix microarray analysis of 132 diagnostic bone marrow aspirates or peripheral blood samples from pediatric patients with leukemia [20] was re-analyzed using the PARTEK genomics suite (PARTEK, St. Louis, MI). One-way analysis of variance was used to identify groups for which differences from ETV6-RUNX1 were significant at $p < 0.05$. MatInspector [21] was used to identify predicted RUNX1 binding sites within the *SPIB* and *POLD1* loci using a 0.8 matrix score cutoff. Multiple alignments of the intron one region of *SPIB* were performed using the CLUSTALW method in Macvector (Accelrys, San Diego, CA). Visualization of published ChIP sequencing data was performed using GALAXY (SPI-B, SRR346333) [22].

Statistical analysis

Statistical analysis was performed using Graphpad Prism 6 (Graphpad, San Diego, CA, USA). Specific statistical tests used are described in the figure legends.

Results

Identification of a RUNX1 site in SPIB *intron 1*

SPIB is expressed at low levels in 12;21 (ETV6-RUNX1) leukemia compared with normal human pre-B cells or other leukemia types [14]. Reanalysis of published microarray data [20] provided further evidence that *SPIB* transcripts were reduced in ETV6-RUNX1 leukemia compared with leukemia associated with MLL, E2A-PBX1, or hyperdiploid chromosomal abnormalities (Fig. 1A). Next, quantitative RT-qPCR analysis, using a standard curve of cloned *GAPDH* and *SPIB* transcripts, was used to measure *SPIB* mRNA levels in REH cells relative to OCI-LY3 and OCI-LY10 diffuse large B-cell lymphoma cells. REH cells have a t (12;21) translocation fusing one RUNX1 and one ETV6 allele, have one intact RUNX1 allele, and have deleted the second ETV6 allele [16]. Quantitative PCR analysis revealed that *SPIB* was expressed at low levels in REH cells relative to OCI-LY3 and OCI-LY10 cells (Fig. 1B). Taken together, these results suggested that *SPIB* might be transcriptionally repressed by ETV6-RUNX1.

To determine if ETV6-RUNX1 can directly interact with the regulatory regions in the *SPIB* locus, MatInspector analysis was used to identify potential RUNX1 interaction sites. We also considered the 3′ half of the *POLD1* gene for RUNX1sites, because the 3′ end of this gene is located less than 1,000 bp away from the first coding exon of *SPIB* (Fig. 1C). A site upstream of

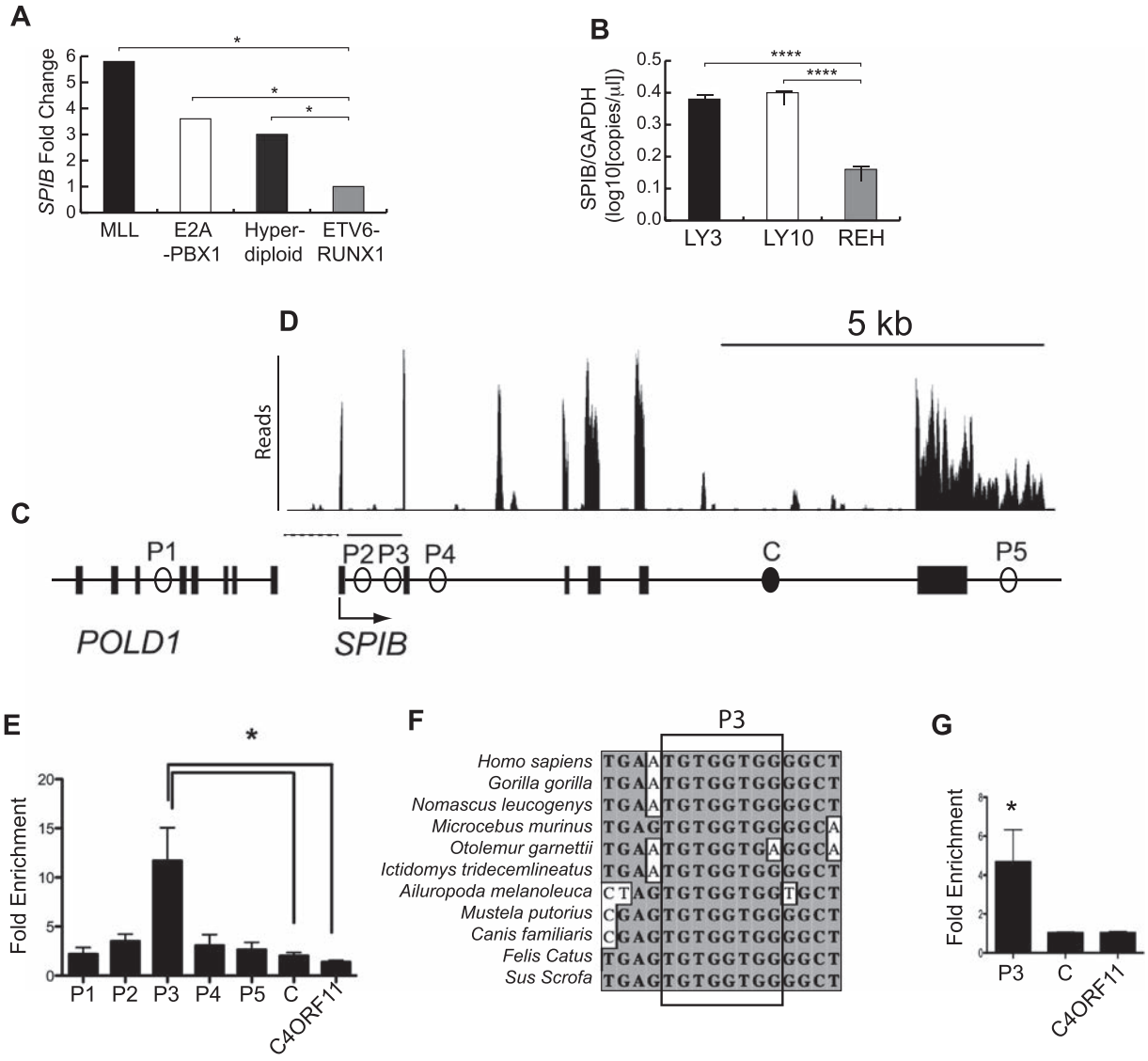

Figure 1. Identification of an ETV6-RUNX1 binding site in *SPIB* intron 1. (**A**) *SPIB* transcripts are expressed at low levels in *ETV6-RUNX1* leukemia. Relative levels of *SPIB* transcripts are represented on the y-axis in RNA samples from 20 *ETV6-RUNX1* leukemia patients compared with 20 samples from three other leukemia subtypes indicated on the x-axis. Statistics were performed using one-way analysis of variance (ANOVA, $*p < 0.05$) (**B**) *SPIB* transcripts are expressed at low levels in REH cells relative to B lymphoma cells. Quantitative PCR using standard curves was used to determine copy numbers of *SPIB* and *GAPDH* mRNA transcript levels in cell lines shown on the x-axis. Statistics were performed using one-way ANOVA ($****p < 0.001$). (**C**) Schematic of the human *SPIB* locus. Exons of the *SPIB* gene and the neighboring *POLD1* gene are indicated as vertical bars. Predicted RUNX1 binding sites located in phylogenetically conserved regions are indicated as circles and labeled P1–P5. The *SPIB* promoter region is indicated by a *thin dotted line,* and intron 1 is indicated by a *thin solid line.* *P* = position. (**D**) RNA sequencing analysis of transcription of the *SPIB* gene in REH cells. (**E**) RUNX1 interacts with P3 in the *SPIB* gene. Chromatin immunoprecipitation analysis was performed using anti-RUNX1 antibody and chromatin prepared from REH cells. Primer sets for qPCR are indicated on the x-axis. Fold enrichment means enrichment using anti-RUNX1 antibody compared with nonspecific IgG antibody. *C4ORF11* is a negative control gene. Statistics were performed using one-way ANOVA for six independent experiments ($*p < 0.05$). (**F**) Multiple-species alignment of the sequence inset of the P3 region. A canonical RUNX1 binding site is marked with a box (**G**) ETV6 interacts with P3 in the *SPIB* gene. ChIP was performed as described for € using anti-ETV6 antibody. Statistics were performed using one-way ANOVA for four independent experiments ($*p < 0.05$).

SPIB exon 1 was confirmed to be a major transcription start site (TSS) in REH cells based on RNA sequencing analysis of this cell line (Fig. 1D) [23]. MatInspector analysis predicted five potential RUNX1 binding sites (numbered position [P] 1–5 in Fig. 1C). To determine if RUNX1 interacts with any of these sites, anti-RUNX1 chromatin immunoprecipitation was performed in REH cells. P3 was more than 12-fold enriched using anti-RUNX1 antibody compared with control IgG antibody (Fig. 1E). P3 was located in *SPIB* intron 1, in a

region that is highly conserved among mammalian species and contained the consensus RUNX1 binding site TGTGGNNN [24] (Fig. 1F). Importantly, anti-ETV6 ChIP indicated that P3 was also associated with ETV6 in REH cells (Fig. 1G). Therefore, RUNX1 or ETV6-RUNX1 protein directly interact with P3 in the *SPIB* gene in REH cells. Taken together, these results suggest that RUNX1 and ETV6-RUNX1 interact with a conserved region at P3 of *SPIB* intron 1.

The RUNX1 binding site in SPIB *intron 1 is repressive in REH cells*

If P3 is a functional binding site for ETV6-RUNX1 in REH cells, then this site would be predicted to be repressive for *SPIB* transcription in REH cells. To test this idea, a conserved 469-bp region of *SPIB* intron 1 encompassing P3 was amplified by PCR, cloned, and ligated upstream of a minimal SV40 promoter driving firefly luciferase (Fig. 2A). Upon transient transfection into REH cells, this reporter vector did not have higher levels of luciferase activity than a vector containing the minimal SV40 promoter alone (Fig. 2B). However, mutation of two nucleotides in the conserved region depicted in Figure 1E (TGTGGTGG → TGTCCTGG), which are known to be required for RUNX1 binding to DNA [24], resulted in significantly higher luciferase activity (Fig. 2B). Next, the function of the 469-bp *SPIB* intron 1 regulatory element was tested in combination with the *SPIB* promoter. A 921-bp segment of the *SPIB* promoter was amplified by PCR, cloned, and ligated into pGL3-basic either alone, in combination with the *SPIB* intron 1 regulatory element, or in combination with the *SPIB* intron 1 RUNX1 mutant element (Fig. 2C). The *SPIB* promoter by itself exhibited significant activity in REH cells compared with the pGL3-basic control (Fig. 2D). Combination of the *SPIB* promoter with the *SPIB* intron 1 regulatory element exhibited no significant enhancement of activity over the *SPIB* promoter alone (Fig. 2D). However, mutation of the RUNX1 binding site in the intron 1 regulatory element resulted in significantly increased luciferase activity (Fig. 2D). Taken together, the results in Figures 2B and 2D suggested that a functional RUNX1 binding site in *SPIB* intron 1 is negatively regulated by ETV6-RUNX1 in REH cells. To test this idea further, SPI-B promoter luciferase reporter vectors were transfected into OCI-LY3 (LY3), an activated B-cell-diffuse large-B-cell lymphoma cell line that does not have an ETV6-RUNX1 translocation and expresses high SPI-B levels as a result of chromosomal translocation to the *SPIB* locus [25]. In LY3 cells, mutation of the RUNX1 binding site in the intron 1 regulatory element did not increase luciferase activity of the SPIB + intron 1 reporter (Fig. 2E). These results suggest that the RUNX1 binding site functions as a negative regulatory element in cells with an ETV6-RUNX1 translocation, but not in other types of malignant cells.

Finally, control experiments were performed to determine whether *SPIB* intron 1 might act as a promoter on its own. *SPIB* intron 1 was ligated into the pGL3-basic luciferase reporter vector and tested for activity in either forward or reverse orientation in REH and LY3 cells. *SPIB* intron 1 did not have detectable transcription activation on its own (Fig. 2F–H). In summary, *SPIB* intron 1 acts as a regulatory element for the *SPIB* promoter that is repressed by ETV6-RUNX1.

Activation of endogenous SPIB *using CRISPRa*

Because SPI-B is a tumor suppressor gene for mouse B-ALL [6,11] and a key activator of gene expression important for B-cell function [7–10], we set out to determine if ectopic expression of SPI-B would be sufficient to alter gene expression in REH cells. The CRISPR-Cas9 system has been adapted for use as a programmable transcriptional regulator, using a nuclease-deactivated Cas9 protein (dCas9) fused to a synthetic VP64 transcriptional activation domain or KRAB transcription repression domain [18,19,26]. dCAS9 protein can be guided to regulatory regions of endogenous target genes using sgRNAs [27]. We recently showed that the transcriptional repressor dCAS9-KRAB could silence endogenous *SPIB* expression in lymphoma cells if directed to an IKAROS binding site located in the first intron [27]. We set out to determine if dCAS9-VP64 could be used to activate endogenous *SPIB* transcription in REH cells.

First, REH cells were infected with a lentiviral vector encoding dCAS9-VP64 [27] and selected for blasticidin resistance (Fig. 3A, *top*). Anti-Cas9 immunoblotting was performed on blasticidin-resistant cells after passage to confirm expression of cCAS9-VP64 protein (Fig. 3B). Next, single guide RNAs (sgRNA) were designed to target the proximal promoter region of *SPIB*. Analysis of ENCODE data [28] suggested that a number of transcription factors target the *SPIB* promoter region (Fig. 3C, *bottom*). Eight sgRNAs were designed to target the proximal promoter region of *SPIB* (Fig. 3C, *top*) and ligated into pU6-sgRNA [27] (Fig. 3A, *bottom*). Plasmid vectors encoding sgRNAs were transfected into REH-dCAS9-VP64 cells using electroporation, in combination with the pGL3-SPIB promoter-luciferase reporter vector, and luciferase activity was measured 24 hours later. With this assay, sgRNA-10 exhibited significant activity (Fig. 3D). Next, pU6-sgRNA10 lentivirus was produced and used to infect REH-dCAS9-VP64 cells. After selection in puromycin, anti-hSPIB immunoblot exhibited increased SPI-B expression (Fig. 3E). Finally, RNA was prepared and used to determine gene expression with RT-qPCR analysis. REH cells expressing sgRNA10 expressed ninefold higher

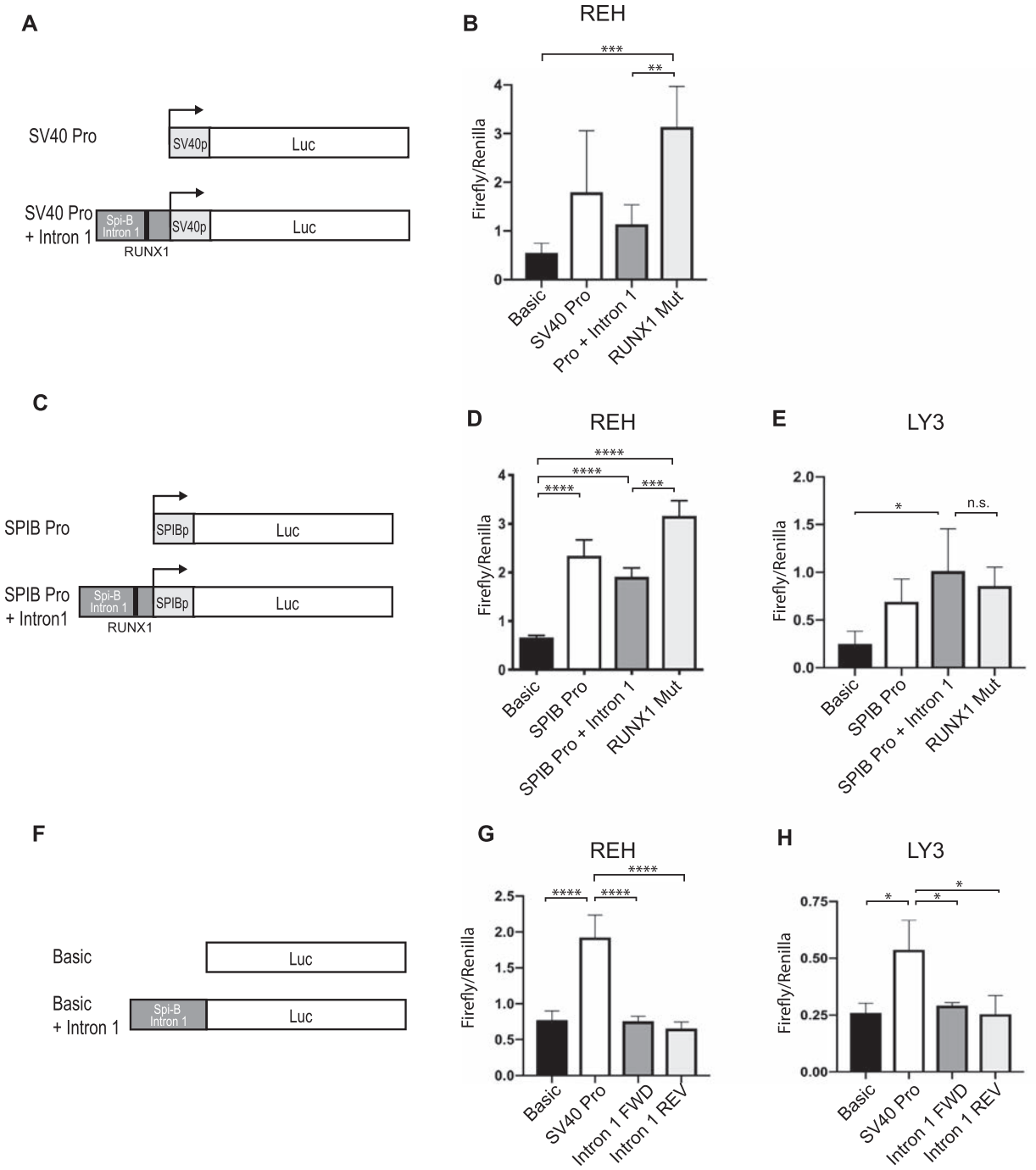

Figure 2. Mutation of a RUNX1 binding site increases transcriptional activation by a regulatory region in *SPIB* intron 1. **(A)** Schematics of luciferase reporter vectors utilizing the SV40 promoter. **(B)** Results of dual luciferase assays expressed as firefly/renilla ratio. Transfections were performed with plasmids including pGL3-basic (Basic), pGL3-SV40p (SV40 Pro), pGL3-SV40p-SPIB-intron 1 (Pro + Intron 1), and pGL3-SV40p-SPIB-intron 1 RUNX1 mutant (RUNX1 Mut). **(C)** Schematics of luciferase reporter vectors utilizing the SPIB promoter. **(D)** Results of dual luciferase assays performed in REH cells expressed as firefly/renilla ratio. Transfections were performed with plasmids including pGL3-basic (Basic), pGL3-SPIBp (SPIB Pro), pGL3-SPIBp-SPIB-intron 1 (SPIB Pro + Intron 1), and pGL3-SPIBp-SPIB-intron 1 RUNX1 mutant (RUNX1 Mut). **(E)** Results of dual luciferase assays performed in LY3 cells expressed as firefly/renilla ratio using the same plasmids as listed for **(D).** **(F)** Schematics of promoterless luciferase reporter vectors utilizing SPIB intron 1. **(G)** Results of dual luciferase assays performed in REH cells expressed as firefly/renilla ratio. Transfections were performed with plasmids including pGL3-basic (Basic), pGL3-SV40p (SV40 Pro), pGL3-SPIB-intron 1 (Intron 1 FWD), and pGL3-SPIB-intron 1 reverse orientation (Intron 1 REV). **(H)** Results of dual luciferase assays performed in LY3 cells expressed as firefly/renilla ratio using the same plasmids as listed for **(G)**. Results are expressed as the mean ± standard deviation. Statistics were performed by one-way ANOVA with Tukey's posttest. $n = 5$.

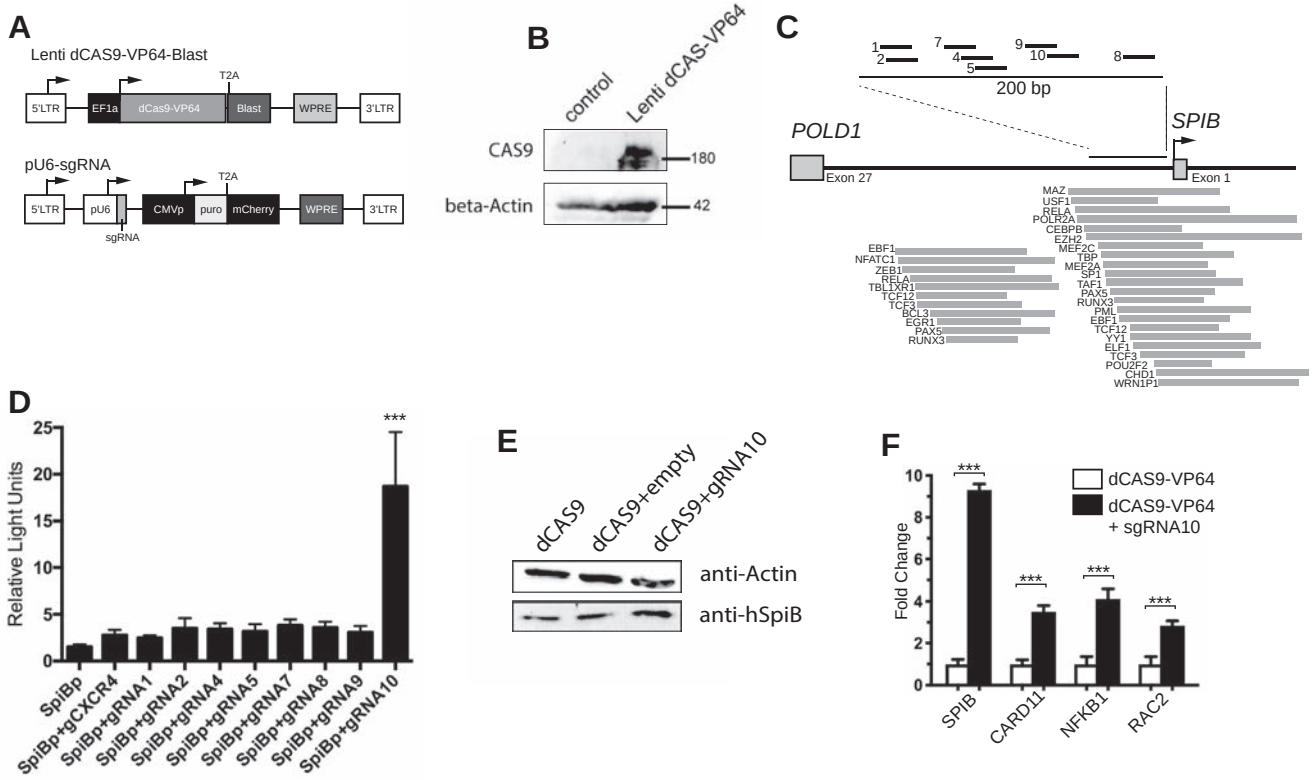

Figure 3. Modulation of gene expression in REH cells by induction of endogenous *SPIB* transcription using CRISPRa. **(A)** Schematic of lentiviral vectors used in this study. **(B)** Anti-Cas9 immunoblot of REH cells infected with Lenti-dCAS9-VP64-blast vector. In the bottom row is an anti-beta-actin immunoblot. **(C)** Schematic showing target site locations of sgRNAs used in this study. The location of ENCODE transcription factors interacting with the *SPIB* promoter region is shown in the lower part of the figure. **(D)** Activation of luciferase activity following transient transfection of pGL3-SPIBp (Fig. 2C) in combination with pU6-sgRNA vectors indicated on the *x*-axis into REH cells. Statistics were performed using one-way ANOVA with Tukey's multiple comparisons test (***$p < 0.001$). **(E)** Increase of endogenous SPI-B protein expression upon infection of REH Lenti-dCAS9-VP64 cells with sgRNA10. The control is an anti-beta-actin immunoblot. **(F)** Induction of endogenous *SPIB* and target gene transcription using sgRNAs 10. On the y-axis is fold induction using *B2M* as a reference gene. Statistics were performed using one-way ANOVA (***$p < 0.001$).

levels of *SPIB* mRNA transcripts than control cells expressing only dCAS9-VP64 (Fig. 3F). *RAC2* and *CARD11* were previously identified as target genes of SPI-B in B cells using a combination of ChIP sequencing and gene expression analyses [22], and we previously identified *Nfkb1* as an activation target of Spi-B in murine B cells [29]. RT-qPCR analysis revealed that mRNA transcript levels of *CARD11, NFKB1*, and *RAC2* were increased in REH cells infected with sgRNA10 (Fig. 3F). In summary, endogenous *SPIB* and target gene expression could be increased using a synthetic transcriptional activator in the t(12;21) cell line REH.

Reduced proliferation in REH cells with ectopic expression of SPI-B or PU.1

Next, we set out to determine if ectopic expression of SPI-B can alter "fitness" in REH cells. Although increased expression of *SPIB* induced by CRISPRa altered gene expression in REH cells, there was no detectable effect on proliferation under standard culture conditions. Therefore, we set out to ectopically express SPI-B at higher levels than could be achieved with CRISPRa. Because PU.1 is highly related to SPI-B and is also a strong transcriptional activator, we also tested ectopic expression of PU.1 in these experiments. We constructed lentiviral vectors encoding 3XFLAG-tagged human SPI-B (pLVX-hSPIB) or PU.1 (pLVX-hPU.1), as well as mutants that are unable to bind DNA (pLVX-hSPIB R229,232A [hSPIB R-A]) or pLVX-hPU.1 R230,233A [hPU.1 R-A]) [30] (Fig. 4A). VSVg-pseudotyped lentivirus was produced with control or cDNA-encoding pLVX vectors and used to infect REH cells. Infected cells were enriched by cell sorting based on ZsGreen expression. After enrichment, REH cells infected with pLVX-SPIB expressed >100-fold higher levels of *SPIB* mRNA than cells infected with pLVX-PU.1, whereas REH cells infected with pLVX-SPIB R-A expressed 50-fold higher levels of *SPIB* mRNA than cells infected with pLVX-PU.1 R-A (Fig. 4B, *left*). REH cells infected with pLVX-PU.1

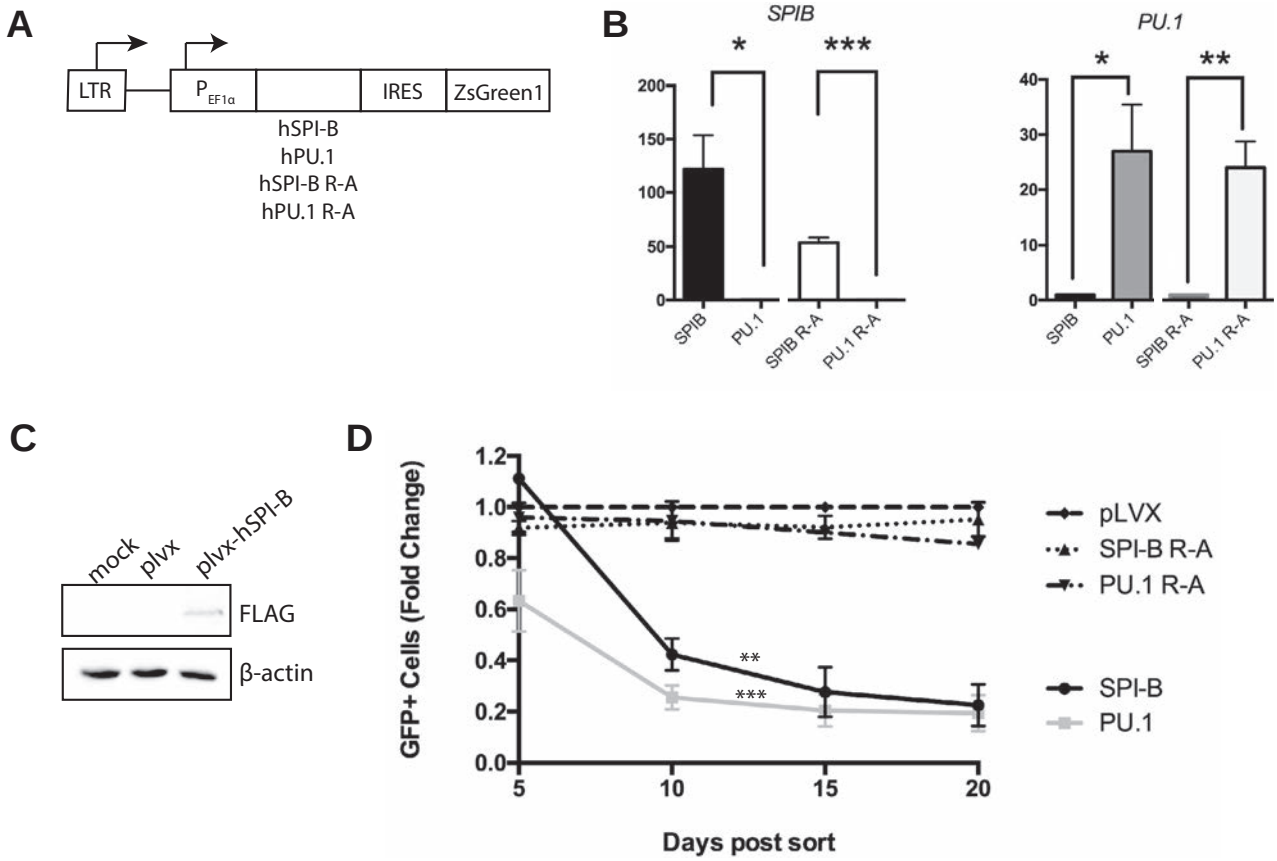

Figure 4. Reduction of REH cell "fitness" on ectopic expression of SPI-B or PU.1. **(A)** Schematic of pLVX-hSPIB and pLVX-hPU.1 vectors. *IRES* = internal ribosome entry site. **(B)** Detection of SPIB or PU.1 mRNA expression following infection. REH cells were infected with pLVX vectors encoding wild-type SPIB (SPIB), wild-type PU.1 (PU.1), SPIB R229, 232A (SPIB R-A), or PU.1 R230, 233A (PU.1 R-A) followed by cell sorting. On the y-axis is fold induction of SPIB (*left*) or PU.1 (*right*) mRNA levels after sort and RNA preparation. Statistics were performed using the *t* test for three independent experiments (*$p < 0.05$, **$p < 0.01$, ***$p < 0.001$). **(C)** Detection of hSPI-B protein using anti-FLAG immunoblot (*top*). An anti-beta-actin immunoblot (*bottom*) was used as control. **(D)** Reduced competitiveness of REH cells upon infection with SPI-B or PU.1. REH cells were infected with vectors indicated in the legend on the right. Infected cells were enriched by cell sorting and placed in culture, and the frequency of GFP^+ cells was determined every 5 days, normalized to the frequency determined at 5 days. Statistics were performed using repeated-measures ANOVA with Dunnett's multiple comparisons test for four independent experiments (**$p < 0.01$, ***$p < 0.001$).

expressed >25-fold higher levels of *SPI1* mRNA than cells infected with pLVX-SPIB, whereas REH cells infected with pLVX-PU.1 R-A expressed 22-fold higher levels of *PU.1-SPI1* mRNA than cells infected with pLVX-SPIB R-A (Fig. 4B, *right*). SPI-B protein was detectable using anti-FLAG immunoblot in pLVX-hSPIB-infected REH cells, but not in control cells (Fig. 4C).

REH cells infected with retroviral vectors were enriched by cell sorting to similar infection frequencies. Enriched cells were placed in culture, and flow cytometry was used to determine frequencies of ZsGreen-expressing cells upon passage at 5-day intervals. Infection with control vector or vectors encoding DNA-binding mutants resulted in sustained GFP expression over 20 days in culture (Fig. 4D). In contrast, infection with SPI-B or PU.1 caused a reduction in the frequency of ZsGreen-expressing cells with each passage, indicating that hSPI-B- or PU.1-infected cells competed poorly with uninfected cells. REH cells infected with SPI-B divided less frequently than cells infected with pLVX control, as determined by CellTrace Violet staining (Supplementary Figure E1, online only, available at www.exphem.org). In summary, ectopic expression of SPI-B or PU.1 reduced proliferation of REH cells relative to control cells.

Induction of apoptosis by PU.1 and SPI-B in REH cells

To determine if increased apoptosis also plays a role in reduced fitness, we determined the difference in frequency of cells in early apoptosis (Annexin V^+, PI^-) or late apoptosis (Annexin V^+ PI^+) for cells infected with SPI-B, PU.1, or mutant SPI-B or PU.1, compared with cells infected with pLVX control vector (gating

strategy illustrated in Fig. 5A). REH cells were infected and enriched for GFP$^+$ cells after 48 hours by cell sorting; then apoptosis was measured after 5 days of culture. Apoptosis was determined as the difference (fold increase) in frequency of apoptotic cells in infected pools of enriched cells relative to pLVX-infected cells. DNA-binding mutants of SPI-B or PU.1 did not induce apoptosis relative to pLVX control vector (Fig. 5B,C). However, infection with SPI-B or PU.1 induced apoptosis in a significant fraction of cells relative to pLVX control (Fig. 5B,C). PU.1 induced the greatest frequency of early (Fig. 5B) and late (Fig. 5C) apoptotic cells after infection. These results suggest that both SPI-B and PU.1 induce increased apoptosis in REH cells, although PU.1 was the more potent inducer of apoptosis.

Modulation of CARD11 *and* CDKN1A *expression by SPI-B and PU.1 in REH cells*

Finally, we set out to determine what target genes might be modulated by ectopic expression of SPI-B or PU.1 to regulate cell cycle progression and apoptosis in REH cells. *CARD11* (encoding caspase recruitment domain/membrane-associated guanylate kinase protein 11) regulates NF-κB pathway-mediated survival of B lymphoma cells [31]. *CARD11* is a direct activation target of SPI-B [22,32]. To determine if *CARD11* is activated by SPI-B or PU.1, we determined mRNA transcript levels after infection with lentiviral vectors encoding SPI-B, PU.1, or DNA-binding mutants of SPI-B and PU.1. RNA was prepared from infected cells enriched by cell sorting for GFP 48 hours after infection. RT-qPCR analysis revealed that *CARD11* was

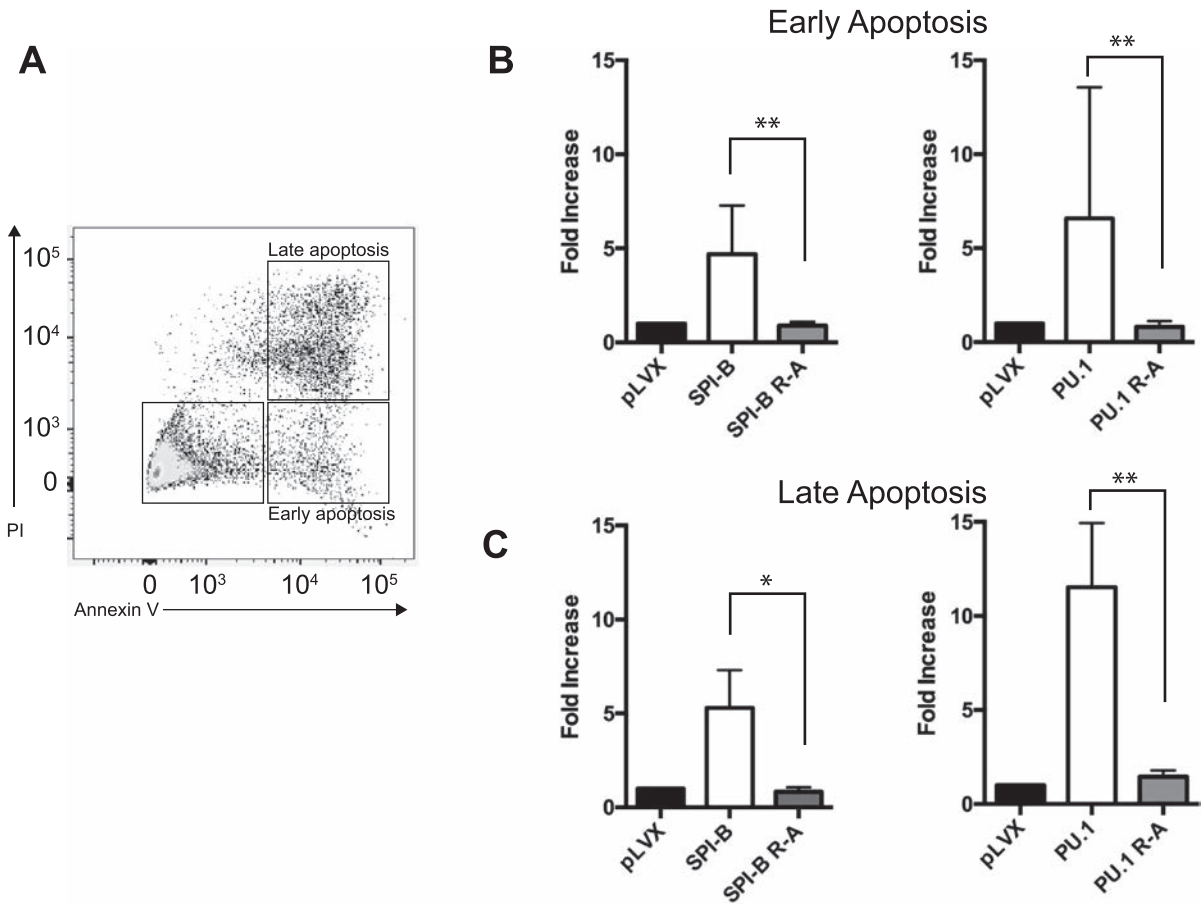

Figure 5. Induction of apoptosis in REH cells upon infection with SPI-B or PU.1. **(A)** Gating strategy for measurement of apoptosis. REH cells were infected with pLVX-hSPI-B before analysis at 48 hours. The plot reveals staining with propidium iodide (PI, y-axis) and Annexin V (x-axis). Boxes indicate gates for no apoptosis (*lower left*), early apoptosis (*lower right*) and late apoptosis (*upper right*). **(B)** SPI-B and PU.1 induce early apoptosis in REH cells. Frequencies of cells in early apoptosis were determined as shown in **(A)** and measured as fold increase compared with pLVX control-infected cells. Statistics were determined using Kruskal–Wallis ANOVA for four independent experiments. **(C)** SPI-B and PU.1 induce late apoptosis in REH cells. Frequencies of cells in late apoptosis were determined as shown in **(A)** and measured as fold increase compared with pLVX control-infected cells. Statistics were determined using the Kruskal–Wallis ANOVA for four independent experiments.

strongly activated by SPI-B and PU.1 in infected REH cells (Fig. 6A).

$P21^{WAF1/Cip1}$ (encoded by *CDKN1A*) is a cyclin-dependent kinase inhibitor that inhibits cell cycle progression [33]. PU.1 has previously been suggested to activate *CDKN1A* transcription to induce cell cycle arrest [34]. In REH cells, PU.1 was found to interact with p53 protein such that knocking down PU.1 led to increased p53-dependent activation of *CDKN1A* transcription and cell cycle arrest [35]. Interestingly, p21 also functions as a regulator of apoptosis, inhibiting apoptosis in most contexts [33]. To determine if p21 is regulated by SPI-B or PU.1, we determined mRNA transcript levels of *CDKN1A* after infection with lentiviral vectors described above. RT-qPCR analysis indicated that *CDKN1A* mRNA transcript levels were reduced by infection with SPI-B or PU.1 relative to DNA binding-domain mutant SPI-B or PU.1 (Fig. 6B). *CDKN1B* (encoding $p27^{Kip1}$) mRNA transcript levels were increased by infection with PU.1, but not changed in response to SPI-B (Fig. 6C). To determine if PU.1 or SPI-B might regulate *CDKN1A* directly, we re-analyzed ChIP sequencing data from HBL1-activated B-cell-diffuse large-B-cell lymphoma cells in which anti-biotag SPI-B ChIP sequencing analysis had been performed [22]. In HBL1 cells, SPI-B interacted strongly with a site in the *CDKN1A* promoter located at position −325 bp from the transcription start site (Fig. 6D). A conserved consensus predicted PU.1/SPI-B binding site (indicated by the asterisk in Fig. 6E) was located at this site, as were two less conserved sites. These results suggest that SPI-B and PU.1 may directly interact with regulatory regions in the *CDKN1A* gene to regulate transcription. Taken together, these results suggest that SPI-B and PU.1 activate *CARD11* and repress *CDKN1A* to modulate cell cycle progression and cell survival in REH cells.

Discussion

In this study, we hypothesized that *SPIB* is directly transcriptionally repressed by ETV6-RUNX1 in t(12;21) leukemia. In support of this hypothesis, we identified a regulatory region in the first intron of *SPIB* that is bound by ETV6-RUNX1 protein in REH cells. Mutagenesis of the RUNX1 binding site in *SPIB* intron 1 prevented transcriptional repression in transient transfection assays. Forced expression of SPI-B, performed using either CRISPR gene activation or ectopic expression with a lentiviral vector, was sufficient to program altered gene expression, impair cell proliferation, and induce apoptosis in REH cells. Finally, we identified *CARD11* and *CDKN1A* as direct transcriptional targets of SPI-B potentially involved in regulation of proliferation and apoptosis. Taken together, this study identifies *SPIB* as an important target of ETV6-RUNX1 in regulation of B-cell gene expression in leukemogenesis.

Fusion of *ETV6* and *RUNX1* genes in t(12;21) leukemia joins a repression domain of ETV6 to the DNA-binding domain of RUNX1 [4]. Genomewide gene expression studies revealed that ETV6-RUNX1 expression results in down-regulation of RUNX1 target genes [36]. Conversely, knockdown of ETV6-RUNX1 leads to upregulation of genes [15]. The widespread epigenetic changes induced by ETV6-RUNX1 lead to expansion of preleukemic B-cell progenitor clones through mechanisms that are poorly understood [37]. Preleukemic ETV6-RUNX1-positive clones acquire secondary cancer driver mutations through a process that is strongly associated with off-target effects of the RAG1/RAG2 recombinase [38]. Secondary driver mutations then synergize with ETV6-RUNX1 to induce leukemogenesis. Thus, ETV6-RUNX1 fusion leads to a clonal evolution process characterized by both epigenetic and genetic changes that results in leukemogenesis.

Three key pieces of information led to the current study. First, *SPIB* is directly activated by RUNX1 during B-cell development [13]. Second, *SPIB* mRNA transcript levels are expressed at low levels in 12;21 (ETV6-RUNX1) leukemia relative to other leukemia subtypes, and at low levels compared with normal human pre-B cells [14]. Third, when RNA interference was used to knock down ETV6-RUNX1 in REH and AT-2 cell lines carrying the 12;21 translocation, *SPIB* was the top upregulated gene [15]. These observations led to our current study in which we showed that ETV6-RUNX1 directly represses *SPIB* transcription through a RUNX1 binding site located in the first intron (Figs. 1 and 2). The RUNX1 binding site is located 42 bp downstream of a functional IKAROS site in *SPIB* intron 1 that functions as an activator of transcription [32]. The close proximity of these two functional binding sites, as well as the identification by the ENCODE project of numerous other transcription factors interacting with this region (Fig. 3C), suggests that this region of *SPIB* intron 1 functions as an important regulatory element. It will be interesting to determine if and how IKAROS and RUNX1 interact to regulate *SPIB* transcription.

Mouse studies using a *Sleeping Beauty* transposase screen in ETV6-RUNX1 knock-in mice reported that *SPIB* mutation strongly cooperated with ETV6-RUNX1 to induce leukemia [6]. An important question is how reduced *SPIB*, caused by either mutation or repression, cooperates with ETV6-RUNX1 to induce human leukemia. Our results indicated that ectopic expression of either SPI-B or PU.1 can lead to altered gene expression, reduced proliferation, and induced apoptosis in REH cells (Figs. 3–6). Because SPI-B is a key activator of gene expression important for B-cell function [7–10], we speculate that ETV6-RUNX1 regulates BCR signaling, B-cell differentiation, apoptosis, and proliferation, at least in part through SPI-B.

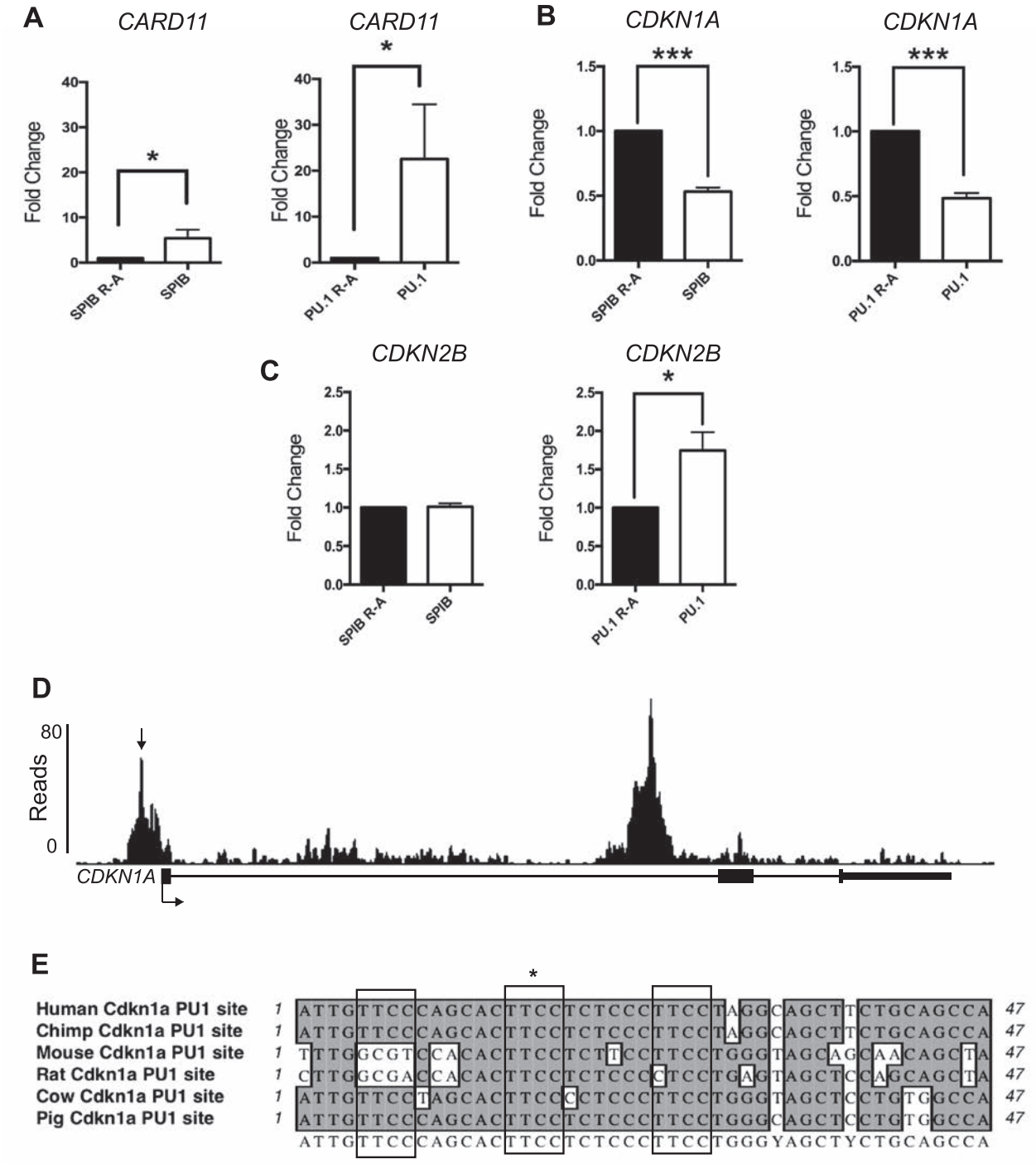

Figure 6. Change in *CARD11* and *CDKN1A* expression by ectopic expression of SPI-B and PU.1. **(A)** Increased *CARD11* expression upon ectopic expression of SPI-B. mRNA levels were normalized to *GAPDH*. **(B)** Reduction of levels of *CDKN1A* mRNA transcripts following infection with SPIB and PU.1. REH cells were infected with pLVX vectors encoding wild-type SPIB (SPIB), wild-type PU.1 (PU.1), SPIB R229, 232A (SPIB R-A), or PU.1 R230, 233A (PU.1 R-A). Forty-eight hours after infection, infected cells were enriched by cell sorting, and RNA was prepared for RT-qPCR analysis. On the y-axis is the fold change in *CDKN1A* mRNA transcript levels. **(C)** Change in levels of *CDKN1B* mRNA transcripts following infection with SPIB and PU.1. The experiment was performed as described above. Statistics were performed using the *t* test (*$p < 0.05$, ***$p < 0.001$). **(D)** Interaction of SPI-B with a site in the human *CDKN1A* promoter. On the y-axis are read counts, and on the x-axis are the locations of aligned reads. **(E)** Identification of a conserved ETS binding site in the *CDKN1A* promoter. Shown is a CLUSTALW alignment of a 47-bp *CDKN1A* promoter fragment centered on the ETS binding site shown in **(C)**.

In our hands, PU.1 was a more potent inhibitor of proliferation (Fig. 4D) and inducer of late apoptosis (Fig. 5) than SPI-B. In addition, PU.1, but not SPI-B, could activate *CDKN1B* expression (Fig. 6B). SPI-B and PU.1 are highly related to one another and occupy many of the same sites in cells in which both proteins are expressed [7]. High expression of PU.1 and Spi-B is tolerated in B lymphoma cells [7], but high expression of PU.1 rapidly induces apoptosis in pro-B cells or murine B-ALL cells [9]. SPI-B and PU.1 function as complementary tumor suppressors, as both genes must be deleted to induce B-ALL in mice [11,14]. However, in ETV6-RUNX1 leukemia, *SPIB* (not PU.1) is expressed at low levels [14]. Therefore, although both SPI-B and PU.1 function as tumor suppressors in B-ALL, reduced expression of *SPIB* likely plays a unique role in cooperating with ETV6-RUNX1 to alter gene expression to a preleukemic state. More work needs to be done to understand differences in biological function between SPI-B and PU.1.

CARD11 (also known as CARMA1) is an essential adaptor protein for BCR signaling to IKK and JNK pathways [39]. In self-reactive B cells, CARD11 is essential for induction of apoptosis upon sustained BCR engagement [40]. Up to 13% of activated B-cell-type diffuse large-B-cell lymphomas were reported to acquire *CARD11* mutations that promote proliferation and survival through the NF-κB pathway, rather than cell death [40,41]. Thus, we speculate that activation of increased levels of CARD11 by SPI-B induces apoptosis through IKK or JNK signaling pathways. CDKN1A is well known to play key roles in both survival and proliferation, and increases and decreases in CDKN1A expression can result in increased apoptosis [33,42]. In conclusion, changes in *CARD11* and *CDKN1A* mRNA transcript levels upon SPI-B transduction are associated with increased apoptosis and decreased proliferation in REH cells. We speculate that altered transcription of *CARD11* and *CDKN1A* is a consequence of ETV6-RUNX1 expression in t(12;21) preleukemic or leukemic cells and is mediated through reduced SPI-B. Changes in *CARD11* and *CDKN1A* mRNA transcript levels upon transduction with SPI-B can be interpreted as evidence of transcriptional programming of REH cells to restore B-cell identity.

Up to two-thirds of leukemias involve mutation or chromosomal translocation of genes encoding transcription factors [2]. Transcription factors have traditionally been considered to be “undruggable” because of their nuclear localization and nonenzymatic mechanism of action. However, recent progress in research has changed this perspective [43]. Chemical inhibitors of histone deacetylases (HDACs) [44] and, more recently, histone acetyltransferases (HATs) [45] show substantial promise in inhibiting tumor growth and inducing differentiation. Progress has also been made in developing drugs that specifically inhibit the activity of ETS-family transcription factors. YK-4-279 inhibits DNA binding of ETS transcription factor family members, including the EWS1-FLI1 fusion protein, to inhibit leukemia [46]. DB2313, DB2115, and DB1976 specifically inhibit binding of PU.1 to DNA, resulting in decreased cell growth and induction of apoptosis of AML cells [47]. Although in the early phases of preclinical or clinical trials, these studies offer hope that transcription factors can be specifically targeted to inhibit growth, induce apoptosis, and promote differentiation of leukemia cells.

In summary, our study suggests that *SPIB* is transcriptionally repressed by ETV6-RUNX1 in 12;21 pre-B-cell acute lymphoblastic leukemia. We found that gene expression in an ETV6-RUNX1 cell line can be significantly altered by endogenous or ectopic expression of SPI-B. These results suggest that reduced transcription of *SPIB* plays a key role in ETV6-RUNX1 programming of developing B cells to a preleukemic state. The gene expression changes that are observed in B-cell progenitors in ETV6-RUNX1 cells [4,5,15] are similar to those induced by deletion of *SPIB* or combined deletion of *SPIB* with *SPI1* [8,9,11]. Determination of the exact role that SPI-B plays in ETV6-RUNX1 leukemia will be an important area of future investigation.

Acknowledgments

This work was supported by a King Abdullah Scholarship to S. Turkistany; an Ontario Trillium grant to Dr. Batista; and grants from the Leukemia and Lymphoma Society of Canada, and the Canadian Institutes of Health Research (Grant Nos. 10651 and 137414) to Dr. DeKoter. We thank Reuben Tooze (University of Leeds, UK) for the gift of the anti-hSPIB antibody used in immunoblot assay. We thank Kristin Chadwick and the London Regional Flow Cytometry Core Facility London, Ontario, Canada for assistance with flow cytometric sorting and analysis. We thank David Carter and the London Regional Genomics Core Facility London, Ontario, Canada for assistance with analysis of microarray data.

References

1. Iacobucci I, Mullighan CG. Genetic basis of acute lymphoblastic leukemia. J Clin Oncol. 2017;35:975–983.
2. Roberts KG, Mullighan CG. Genomics in acute lymphoblastic leukaemia: insights and treatment implications. Nat Rev Clin Oncol. 2015;12:344–357.
3. Hong D, Gupta R, Ancliff P, et al. Initiating and cancer-propagating cells in TEL-AML1-associated childhood leukemia. Science. 2008;319:336–339.
4. Zelent A, Greaves M, Enver T. Role of the TEL-AML1 fusion gene in the molecular pathogenesis of childhood acute lymphoblastic leukaemia. Oncogene. 2004;23:4275–4283.

5. Tsuzuki S, Seto M, Greaves M, Enver T. Modeling first-hit functions of the t(12;21) TEL-AML1 translocation in mice. Proc Natl Acad Sci USA. 2004;101:8443–8448.
6. van der Weyden L, Giotopoulos G, Rust AG, et al. Modeling the evolution of ETV6-RUNX1-induced B-cell precursor acute lymphoblastic leukemia in mice. Blood. 2011;118:1041–1051.
7. Solomon LA, Li SKH, Piskorz J, Xu LS, DeKoter RP. Genome-wide comparison of PU.1 and Spi-B binding sites in a mouse B lymphoma cell line. BMC Genom. 2015;16:76.
8. Xu LS, Sokalski KM, Hotke K, et al. Regulation of B cell linker protein transcription by PU.1 and Spi-B in murine B cell acute lymphoblastic leukemia. J Immunol. 2012;189:3347–3354.
9. Christie DA, Xu LS, Turkistany SA, et al. PU.1 Opposes IL-7-dependent proliferation of developing B cells with involvement of the direct target gene bruton tyrosine kinase. J Immunol. 2015;194:595–605.
10. Bunting KL, Soong TD, Singh R, et al. Multi-tiered reorganization of the genome during B cell affinity maturation anchored by a germinal center-specific locus control region. Immunity. 2016;45:497–512.
11. Sokalski KM, Li SK, Welch I, Cadieux-Pitre HA, Gruca MR, DeKoter RP. Deletion of genes encoding PU.1 and Spi-B in B cells impairs differentiation and induces pre-B cell acute lymphoblastic leukemia. Blood. 2011;118:2801–2808.
12. Batista CR, Lim M, Laramee AS, et al. Driver mutations in Janus kinases in a mouse model of B-cell leukemia induced by deletion of PU.1 and Spi-B. Blood Adv. 2018;2:2798–2810.
13. Niebuhr B, Kriebitzsch N, Fischer M, et al. Runx1 is essential at two stages of early murine B-cell development. Blood. 2013;122:413–423.
14. Pang SH, Minnich M, Gangatirkar P, et al. PU.1 cooperates with IRF4 and IRF8 to suppress pre-B-cell leukemia. Leukemia. 2016;30:1375–1387.
15. Fuka G, Kauer M, Kofler R, Haas OA, Panzer-Grumayer R. The leukemia-specific fusion gene ETV6/RUNX1 perturbs distinct key biological functions primarily by gene repression. PLoS One. 2011;6:e26348.
16. Uphoff CC, MacLeod RA, Denkmann SA, et al. Occurrence of TEL-AML1 fusion resulting from (12;21) translocation in human early B-lineage leukemia cell lines. Leukemia. 1997;11:441–447.
17. Yee C, Biondi A, Wang XH, et al. A possible autocrine role for interleukin-6 in two lymphoma cell lines. Blood. 1989;74:798–804.
18. Gilbert LA, Horlbeck MA, Adamson B, et al. Genome-scale CRISPR-mediated control of gene repression and activation. Cell. 2014;159:647–661.
19. Konermann S, Brigham MD, Trevino AE, et al. Genome-scale transcriptional activation by an engineered CRISPR−Cas9 complex. Nature. 2015;517:583–588.
20. Ross ME, Zhou X, Song G, et al. Classification of pediatric acute lymphoblastic leukemia by gene expression profiling. Blood. 2003;102:2951–2959.
21. Cartharius K, Frech K, Grote K, et al. MatInspector and beyond: promoter analysis based on transcription factor binding sites. Bioinformatics. 2005;21:2933–2942.
22. Yang Y, Shaffer AL III, Emre NC, et al. Exploiting synthetic lethality for the therapy of ABC diffuse large B cell lymphoma. Cancer Cell. 2012;21:723–737.
23. Ghazavi F, De Moerloose B, Van Loocke W, et al. Unique long non-coding RNA expression signature in ETV6/RUNX1-driven B-cell precursor acute lymphoblastic leukemia. Oncotarget. 2016;7:73769–73780.
24. Melnikova IN, Crute BE, Wang S, Speck NA. Sequence specificity of the core-binding factor. J Virol. 1993;67:2408–2411.
25. Lenz G, Nagel I, Siebert R, et al. Aberrant immunoglobulin class switch recombination and switch translocations in activated B cell-like diffuse large B cell lymphoma. J Exp Med. 2007;204:633–643.
26. La Russa MF, Qi LS. The new state of the art: Cas9 for gene activation and repression. Mol Cell Biol. 2015;35:3800–3809.
27. Gilbert LA, Larson MH, Morsut L, et al. CRISPR-mediated modular RNA-guided regulation of transcription in eukaryotes. Cell. 2013;154:442–451.
28. Davis CA, Hitz BC, Sloan CA, et al. The encyclopedia of DNA elements (ENCODE): Data portal update. Nucleic Acids Res. 2018;46:D794–D801.
29. Li SK, Abbas AK, Solomon LA, Groux GM, DeKoter RP. Nfkb1 activation by the E26 transformation-specific transcription factors PU.1 and Spi-B promotes Toll-like receptor-mediated splenic B cell proliferation. Mol Cell Biol. 2015;35:1619–1632.
30. Houston IB, Huang KJ, Jennings SR, DeKoter RP. PU.1 immortalizes hematopoietic progenitors in a GM-CSF-dependent manner. Exp Hematol. 2007;35:374–384. e1.
31. Bertin J, Wang L, Guo Y, et al. CARD11 and CARD14 are novel caspase recruitment domain (CARD)/membrane-associated guanylate kinase (MAGUK) family members that interact with BCL10 and activate NF-kappa B. J Biol Chem. 2001;276:11877–11882.
32. Solomon LA, Batista CR, DeKoter RP. Lenalidomide modulates gene expression in human ABC-DLBCL cells by regulating IKAROS interaction with an intronic control region of SPIB. Exp Hematol. 2017;56:46–57. e1.
33. Abbas T, Dutta A. p21 in cancer: intricate networks and multiple activities. Nat Rev Cancer. 2009;9:400–414.
34. Yuki H, Ueno S, Tatetsu H, et al. PU.1 is a potent tumor suppressor in classical Hodgkin lymphoma cells. Blood. 2013;121:962–970.
35. Tschan MP, Reddy VA, Ress A, Arvidsson G, Fey MF, Torbett BE. PU.1 binding to the p53 family of tumor suppressors impairs their transcriptional activity. Oncogene. 2008;27:3489–3493.
36. Teppo S, Laukkanen S, Liuksiala T, et al. Genome-wide repression of eRNA and target gene loci by the ETV6-RUNX1 fusion in acute leukemia. Genome Res. 2016;26:1468–1477.
37. Alpar D, Wren D, Ermini L, et al. Clonal origins of ETV6-RUNX1(+) acute lymphoblastic leukemia: studies in monozygotic twins. Leukemia. 2015;29:839–846.
38. Papaemmanuil E, Rapado I, Li Y, et al. RAG-mediated recombination is the predominant driver of oncogenic rearrangement in ETV6-RUNX1 acute lymphoblastic leukemia. Nat Genet. 2014;46:116–125.
39. Jun JE, Wilson LE, Vinuesa CG, et al. Identifying the MAGUK protein Carma-1 as a central regulator of humoral immune responses and atopy by genome-wide mouse mutagenesis. Immunity. 2003;18:751–762.
40. Jeelall YS, Wang JQ, Law HD, et al. Human lymphoma mutations reveal CARD11 as the switch between self-antigen-induced B cell death or proliferation and autoantibody production. J Exp Med. 2012;209:1907–1917.
41. Lenz G, Davis RE, Ngo VN, et al. Oncogenic CARD11 mutations in human diffuse large B cell lymphoma. Science. 2008;319:1676–1679.
42. Ford AM, Palmi C, Bueno C, et al. The TEL-AML1 leukemia fusion gene dysregulates the TGF-beta pathway in early B lineage progenitor cells. J Clin Invest. 2009;119:826–836.
43. Takei H, Kobayashi SS. Targeting transcription factors in acute myeloid leukemia. Int J Hematol. 2018. https://doi.org/10.1007/s12185-018-2488-1.

44. Khan O, La Thangue NB. HDAC inhibitors in cancer biology: emerging mechanisms and clinical applications. Immunol Cell Biol. 2012;90:85–94.
45. Lasko LM, Jakob CG, Edalji RP, et al. Discovery of a selective catalytic p300/CBP inhibitor that targets lineage-specific tumours. Nature. 2017;550:128–132.
46. Minas TZ, Han J, Javaheri T, et al. YK-4-279 effectively antagonizes EWS-FLI1 induced leukemia in a transgenic mouse model. Oncotarget. 2015;6:37678–37694.
47. Antony-Debre I, Paul A, Leite J, et al. Pharmacological inhibition of the transcription factor PU.1 in leukemia. J Clin Invest. 2017;127:4297–4313.

Supplementary Table 1. Primer Sequences

Name	Sequence
1) qPCR Primers	
SPIB qPCR forward	5′-TTACCGTTGGACAGCCCTGC-3′
SPIB qPCR reverse	5′-AGCTTCTTGCGAGTCCCTGC-3′
GAPDH qPCR forward	5′-CATGTTCGTCATGGGTGTGAACCA-3′
GAPDH qPCR reverse	5′-AGTGATGGCATGGACTGTGGTCAT-3′
GAPDH RT-qPCR forward	5′-CATGTTCGTCATGGGTGTGAACCA-3′
GAPDH RT-qPCR reverse	5′-AGTGATGGCATGGACTGTGGTCAT-3′
B2M RT-qPCR forward	5′-TGACTTTGTCACAGCCCAAGA -3′
B2M RT-qPCR reverse	5′-TCCAAATGCGGCATCTTCAAA-3′
SPIB RT-qPCR forward	5′-TCGACGGGCCACACTTCA-3′
SPIB RT-qPCR reverse	5′-TGAATCAGGGTAGCTGGAATGC-3′
CARD11 RT-qPCR forward	5′-GAAAGCGCTTCTTCTGGCTG-3′
CARD 11 RT-qPCR reverse	5′-AGCTCCTCCTGGTGAAACTG-3′
RAC2 RT-qPCR forward	5′-CGACAAGGACACCATCGAGAA-3′
RAC2 RT-qPCR reverse	5′-GCACTCCAGGTATTTCACCG-3′
NFkB1 RT-qPCR forward	5′-GCTTAGGAGGGAGAGCCCA-3′
NFkB1 RT-qPCR reverse	5′-CTTCTGCCATTCTGAAGCCG-3′
P21 RT-qPCR forward	5′-TGCCGAAGTCAGTTCCTTGTGG-3′
P21 RT-qPCR reverse	5′-GTTCTGACATGGCGCCTCC-3′
P27 RT-qPCR forward	5′-CTTGCCCGAGTTCTACTACAGACC-3′
P27 RT-qPCR reverse	5′-GTCCTCAGAGTTAGCCGGAGC-3′
2) ChIP qPCR Primers	
P1 ChIP forward	5′-TGGTGAAGCAGTGGAAAGAGTC-3′
P1 ChIP reverse	5′-AGACCAGGATGAGCTCTTAGGG-3′
P2 ChIP forward	5′-CCACCTGCACTGCCCCTC-3′
P2 ChIP reverse	5′-TGGACCCCTCCCCTCCAC-3′
P3 ChIP forward	5′-GAGTCCGGTGAATGTGGTGG-3′
P3 ChIP reverse	5′-CTGGAGGGGGAGAGACACAG-3′
P4 ChIP forward	5′-CGGAATACTATACCCAACACCCTTG-3′
P4 ChIP reverse	5′-GCATAAACAGGGGCTTTCTTTCAA-3′
P5 ChIP forward	5′-AAAACAATTAGCCGAGCGTGG-3′
P5 ChIP reverse	5′-ACAGCTCACTACAGCCTCCTA-3′
C (Control) ChIP forward	5′-AGGCATGATGGTGCATACTTGT-3′
C (Control) ChIP reverse	5′-TTTTTCAAGGCAGGGTCTCGTT-3′
C4ORFII ChIP forward	5′-GTATTCAGCCAGCCTTTTCTTGG-3′
C4ORFII ChIP forward	5′-ACACAGCTTATCTCAAGGTGACA-3′
3) Site Directed Mutagenesis Primers	
CXCR4 deletion forward	5’-TTTTAGACTAGAAATAGCAAG-3’
CXCR4 deletion reverse	5’-CAACAAGGTGGTTCTCCAAG-3’
RUNX1 Site A Mut forward	5′-GACATTCACCGGACTCCCCCAC-3′
RUNX1 Site A Mut reverse	5′-CTGGGGCTGGTCCCTCACACAG-3′
SPIB R229,232A forward	5′-CTCGCAAACTACGCCAAGACCGGC-3′
SPIB R229,232A reverse	5′-GGCGGCCGCCAGCTTCTGGTAGGTC-3′
PU.1 R230,233A forward	5′-CTGGCCAACTACGGCAAGACGGGC-3′
PU.1 R230,233A reverse	5′-CGCGGCCGCCATCTTCTGGTAGGTC-3′
4) SGRNA Sequences	
sgRNA10	5′-GTGCCCGCTGGCCACAAGCTG-3′
5) Other Cloning Primers	
SPIB qPCR template forward	5′-AGAACTTCGCTAGCCAGACCCTG-3′
SPIB qPCR template reverse	5′-AGGAGTTCCTTGTGCTTGGAGGA-3′
GAPDH qPCR template forward	5′-AAGGTCGGAGTCAACGGATTTGGT-3′
GAPDH qPCR template reverse	5′-ACAAAGTGGTCGTTGAGGGCAATG-3′
SPIB intron 1 cloning forward (KpnI)	5′-ACGTGGTACCACTCTCAGTGCCTCCATCTGG-3′
SPIB intron 1 cloning reverse (MulI)	5′-ACGTACGCGTCTGAATCTCAAAGTGGTTGGGGGCTG-3′
SPIB promoter cloning forward (XhoI)	5′-ACGTCTCGAGGGTGCTTTGTGGTCTCTGGGGGAC-3′
SPIB promoter cloning reverse (BglII)	5′-ACGTAGATCTGCCCGCTGCAGCCG-3′
SP-dCas9-VPR FWD Primer (with NotI restriction site)	5′-AGGCGGCCGCCTCGTTTAGTGAACCGTCAGAT-3′
SP-dCas9-VPR REV Primer	5′-CCCGTTTAAACTCAT ACTAACCGGTAGGG-3′

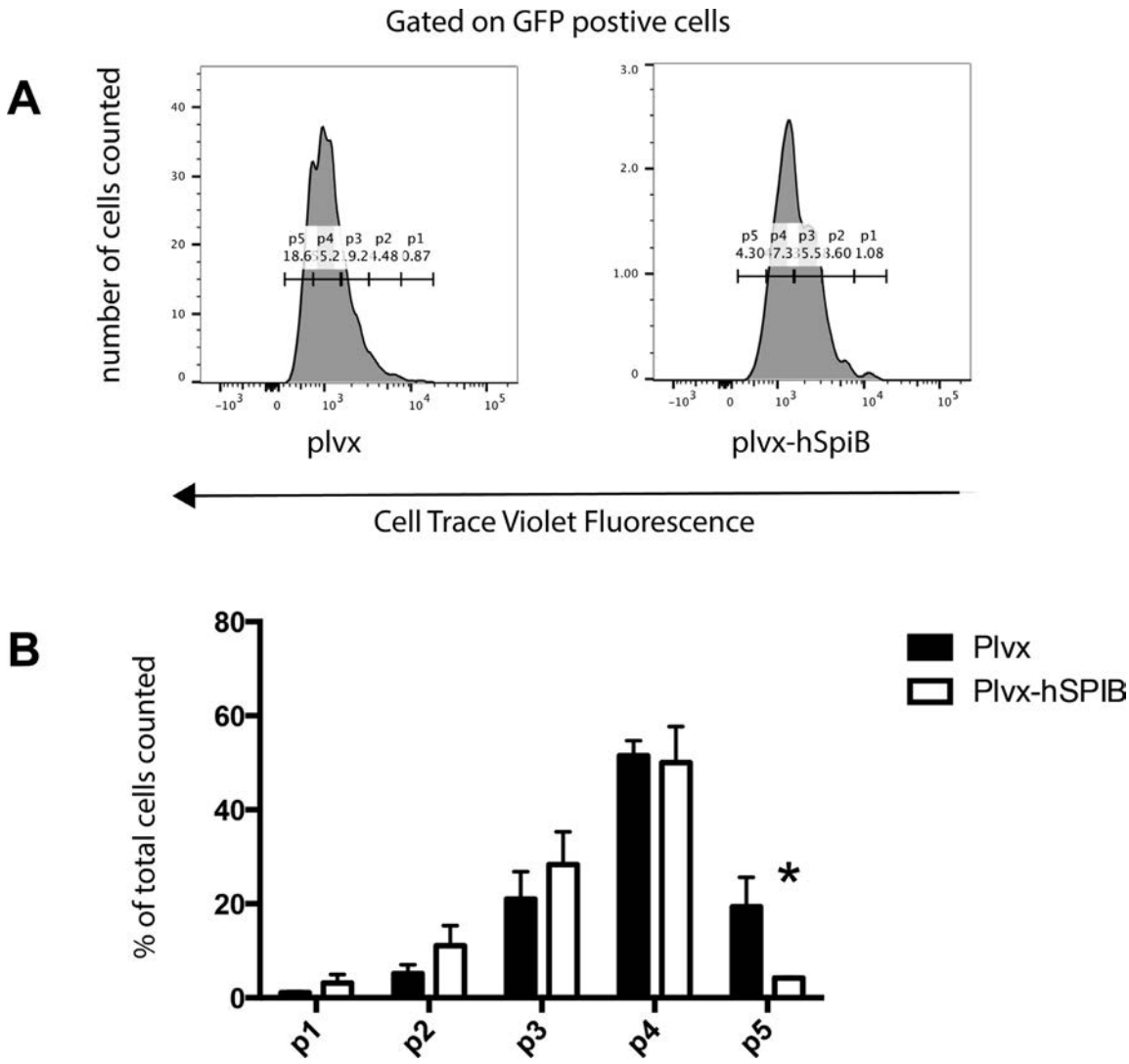

Supplementary Figure 1. Reduced proliferation of REH cells expressing high SPI-B levels. REH cells infected with pLVX control or pLVX-hSPI-B retroviral vectors were loaded with CellTrace Violet and placed in culture for 5 days before flow-cytometric analysis. (**A**) Representative histograms demonstrating gating strategy. P1-P5 represent numbers of cell divisions. (**B**) SPI–infected REH cells show reduced cell division at P5. Asterix represents $p<0.05$ measured by unpaired *t*-test for 3 independent experiments.